INSTITUTE OF PHYSICS PUBLISHING SEMICONDUCTOR SCIENCE AND TECHNOLOGY

Semicond. Sci. Technol. **22** (2007) 97–102 doi:10.1088/0268-1242/22/2/016

The effect of high-frequency sonication on charge carrier transport in LPE and MBE HgCdTe layers

R K Savkina, A B Smirnov and F F Sizov

V Lashkaryov Institute of Semiconductor Physics, National Academy of Sciences of Ukraine, pr. Nauki 45, 03028, Kiev, Ukraine

E-mail: alex_tenet@rambler.ru

Received 28 August 2006, in final form 2 November 2006
Published 19 December 2006
Online at stacks.iop.org/SST/22/97

Abstract

A systematic study of mercury cadmium telluride thin films subjected to high-frequency sonication was carried out. Photoconductivity spectroscopy and the Hall effect technique were used. The charge carrier transport parameters were determined from the Hall coefficient and conductivity measurements. The best agreement between experiment and calculation was obtained assuming that the layer with low-mobility electrons was formed as a consequence of the sonication. It was also determined that the parameters of HgCdTe thin films grown by MBE on GaAs substrates are stable to ultrasonic influence, whereas for HgCdTe thin films grown by LPE on CdZnTe substrates the conductivity-type conversion stimulated by sonication takes place. Substrate properties have been observed to play a significant role for the stability of the HgCdTe epilayers. The phenomenon of the negative differential resistance was detected during the sonication of the n-type HgCdTe bulk crystal.

1. Introduction

$Hg_{1-x}Cd_xTe$ (MCT) remains the most widely used variable gap semiconductor for IR photodetectors despite numerous attempts to replace it with alternative materials. This follows both from fundamental considerations and the material flexibility. At present efforts in infrared detector research are directed towards improving the performance of single element devices, large electronically scanned arrays and higher operating temperature [1]. At the same time the parameter stability of the most used for FPA arrays MCT epitaxial layers under the external action is an important factor of reliability of the infrared FPA detectors.

It is known that MCT alloys exhibit an unusual sensitivity to deformations and mechanical stresses, which accompany the device manufacturing, induce high density of structural defects and dramatically change of the device quality. In this connection we suppose that the use of the high-frequency acoustic vibrations is a good tool for driving material into the high non-equilibrium state for the purpose of studying the material properties change stimulated by deformations.

In the present work we report on studies of the electrical properties of MCT epilayers subjected to high-frequency sonication.

2. Experiment

We have carried out a systematic study of mercury cadmium telluride thin films for 8–12 μm spectral region FPAs which were grown by liquid-phase epitaxy (LPE) and molecular-beam epitaxy (MBE) methods. MBE MCT epitaxial layers were grown on 2-inch diameter (013) GaAs substrates with an intermediate CdZnTe buffer layer [2]. The growth temperature was within $T = 240$–300 °C for CdZnTe buffer layers and within $T \approx 180$–190 °C for the MCT layers. During the growth process, the composition of the layer was controlled by a built-in ellipsometer. The composition non-uniformity over the area of about 1 cm^2 did not exceed $\Delta x = \pm 0.001$. The as-grown layers were of n-type conductivity and p-type MCT layers were obtained by annealing at 200–300 °C. Semi-insulating $Cd_{1-x}Zn_xTe$ ($x = 0.04$) wafers were used as substrates for LPE-grown p-type MCT layers.

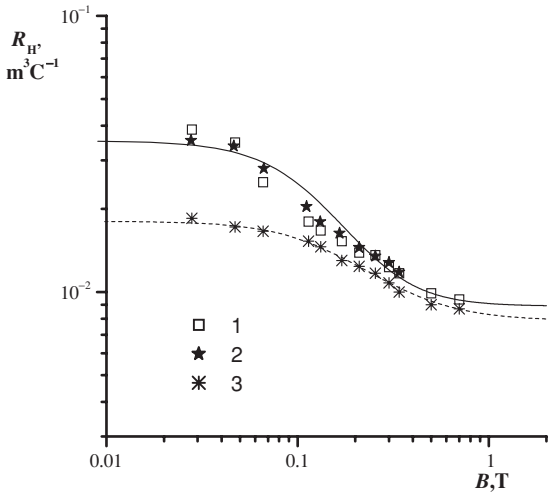

Figure 1. Magnetic field dependences of the Hall coefficient for the typical MBE-grown n-type $Hg_{1-x}Cd_xTe$ layer, $T = 78$ K. Curve 1—initial, curves 2, 3 —after the 1st and 2nd sonication, respectively. Solid lines present the results of the fitting procedure.

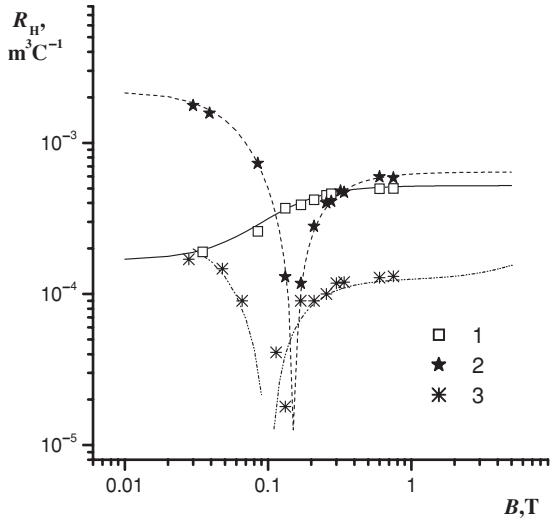

Figure 2. Magnetic field dependences of the Hall coefficient for the typical LPE-grown p-type $Hg_{1-x}Cd_xTe$ layer, $T = 78$ K. Curve 1—initial, curves 2, 3—after 1st and 2nd sonication, respectively. Solid lines present the results of the fitting procedure.

Samples 1 × 1 cm in size were cut for measurements from wafers. An optical microscope was used to determine the thickness of grown layers, which was from 10 μm to 20 μm.

The concentration and mobility of carriers in MCT layers were determined from the Hall coefficient R_H and conductivity σ measurements which were made by the van der Pauw method in the magnetic field B of 0.01 up to 0.7 T at $T = 78$ °K. The high resistivity of the substrates excluded any influence on the results of electrical measurements. A standard procedure of photoconductivity spectroscopy was also employed prior to and after the sonication.

MCT thin films were treated for 30 min at room temperature by longitudinal ultrasonic (US) vibrations with frequency $f_{US} = 7.5$ MHz and intensity $W_{US} < 10^4$ W m^{-2} excited by a $LiNbO_3$ piezo-transducer. It was applied the subthreshold-intensity conditions of US treatment, which results in transformation of already existing structure defects and does not cause the generation of dislocations [3].

3. Results

The magnetic-field dependences of the Hall coefficient and the conductivity were measured. The change of the measurable parameters after sonication was observed for all samples. Figures 1 and 2 show the typical field dependence of the Hall coefficient for MCT films investigated. Points in the figures represent the experimental Hall effect data, and lines are the result of calculations. The Hall effect data were processed in terms of the model, which includes several kinds of carriers using the following expression [4]:

$$eR_H(B) = \frac{\sum a_i \mu_i c_i(B)}{\left(\sum c_i(B)\right)^2 + B^2 \left(\sum a_i \mu_i c_i(B)\right)^2}$$

where e is the electric charge, $c_i = n_i\mu_i/(1+\mu_i^2B^2)$, n_i is the concentration of the ith type of carrier, μ_i is the mobility of the ith type of carrier, a_i is the sign of the carrier (−1 for electrons, +1 for holes) and B is the magnetic flux density. In addition, the zero magnetic field electrical conductivity is given by $\Sigma(0) = e\Sigma c_i(0)$. From the analysis carried out the electron and hole concentration and mobility were obtained before and after ultrasonic treatment (see table 1).

In MBE-grown p-type MCT layers the initial values of the Hall coefficient R_H and conductivity σ are independent of the magnetic field intensity B. This indicates that only carriers of a single kind are present. After sonication hole concentration increase and mobility decrease are observed (see table 1, sample 1).

In MBE-grown n-type MCT layers the initial value of the Hall coefficient R_H is dependent on the magnetic field B (see figure 1). Attempts to describe the experimental data using one carrier type (electron) or using combined electron and hole conductivity and also taking into account the light hole contribution were equally unsuccessful. The Hall effect data were satisfactorily explained by using two types of electrons of vastly different mobility and concentration as well as considering the field dependence of the conductivity $\sigma(B)$. Moreover, 'heavy' electrons are localized in the conducting layer with characteristic dimension d_{1layer}. The calculated values of the charge carrier parameters and d_{1layer} are presented in table 1 (sample 2). After sonication a tendency to electron concentration increase and mobility decrease is observed.

The initial field dependence of the Hall coefficient of the typical LPE-grown p-type MCT layer is shown in figure 2 (curve 1). The concentration and mobility of majority carriers for this sample are presented in table 1 (sample 3). After sonication the change of the conductivity type p → n at a low magnetic field took place (see figure 2, curve 2). A fitting procedure to the experimental data was applied in this case too. The best agreement between experimental and calculated $R_H(B)$ dependences was obtained assuming that the layer with n-type conductivity was formed as a consequence of the sonication. The layer characteristic dimension d_{1layer} and charge carrier parameters were determined (see table 1).

Table 1. Some parameters of typically investigated $Hg_{1-x}Cd_xTe$ epilayers, $T = 78$ K. The parameters n_d and μ_{nd} are the concentration and mobility of 'heavy' electrons.

Sample	p cm^{-3}	μ_p, cm^2 V^{-1} c^{-1}	n, cm^{-3}	μ_n, cm^2 V^{-1} c^{-1}	n_d, cm^{-3}	μ_{nd}, cm^2 V^{-1} c^{-1}	d_{layer}, μm	ρ, $\Omega \cdot$ cm	
1									
MBE	8×10^{15}	373	–	–	–	–	–	2.1	Initial
$x = 0.22$	9×10^{15}	360	–	–	–	–	–	1.9	1st sonication
$d = 12$ μm	16×10^{15}	247	–	–	–	–	–	1.56	2nd sonication
2									
MBE	–	–	2.3×10^{13}	84 500	1.8×10^{15}	8000	1.5	1.87	Initial
$x = 0.21$	–	–	2.3×10^{13}	84 500	1.8×10^{15}	8000	1.5	1.85	1st sonication
$d = 14$ μm	–	–	2.5×10^{13}	70 000	2.1×10^{15}	5800	2.8	1.6	2nd sonication
3									
LPE	1.2×10^{16}	511	3×10^{11}	85 000	–	–	–	0.89	Initial
$x = 0.2$	1.1×10^{16}	320	3.3×10^{11}	120 000	2×10^{14}	1000	2.28	1.6	1st sonication
$d = 19$ μm	3.5×10^{16}	222	10^{11}	140 000	3×10^{15}	1000	4.8	0.54	2nd sonication

4. Discussion

Thus, we have demonstrated that the action of the acoustic wave excited in MCT epilayers by a piezo-transducer results in a change of the carrier transport up to the change of the conductivity type.

4.1. Parameter stability of MCT thin films.

Experimental data from table 1 clearly shows that the parameters of MCT thin films grown by MBE are more stable to the sonication than MCT thin films grown by LPE. For MBE samples, a change of the charge carrier mobility and concentration took place only after the second US treatment. The radiation hardness of similar MBE MCT films [5] and MCT-based photodiodes [6] should also be noted.

Previously, the correlation between the density of extended defects and the value of the sonically stimulated effects for bulk MCT crystals has been found [7]. We have a multilayer system. The structural perfection of the epilayer strongly depends on the conformity between the crystal parameters of the substrate and the layer. At first sight, the highest crystal perfection is realized for MCT layers on lattice matched CdZnTe substrates in contrast to the high defect density generation due to a large lattice mismatch for MCT layers on GaAs substrates. As determined by the etch pit density method, the dislocation density in MBE-grown MCT films was about 10^6 cm^{-2}. For LPE-grown MCT films, this value did not exceed 10^5 cm^{-2}. Thus, their parameters have to be more resistant to US influence. But it seems that other factors play the key role here.

In our experiment the ultrasonic wavelength amounts to ~400–700 μm and exceeds the thickness of epilayers essentially. In other words, the wave propagation process and energy dissipation have taken place mainly in the substrate. According to [8], where the authors have investigated the stability of the CdTe epilayer parameters against ageing and acoustic treatments, acoustic vibrations of the sub-threshold power level stimulate the dissociation of defect complexes in the substrate material, resulting in an increase in the concentration of mobile defects and their diffusion from the substrate to the epilayer. Hence, it could be expected that the sonically stimulated processes at the substrate do have considerable influence on the stability of epilayer parameters.

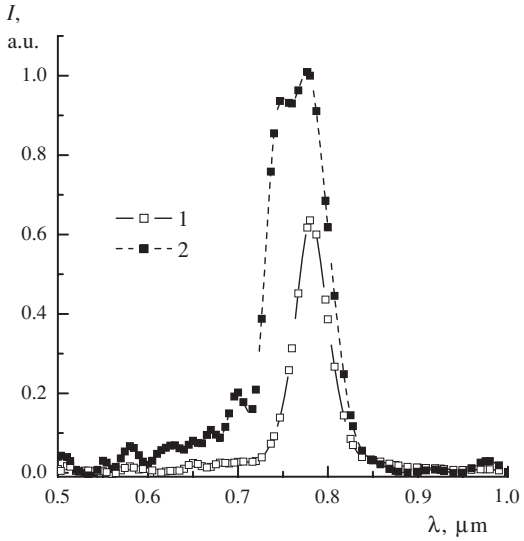

Figure 3. Curves of the photocurrent spectral response for $Cd_{1-x}Zn_xTe$ substrates before (curve 1) and after (curve 2) sonication, $T = 78$ K.

To check the above assumption we have investigated the spectral response of the photocurrent both for MBE-grown and for LPE-grown structures illuminated from the substrate side before and after sonication. We also controlled the photosensitivity of MCT epilayers illuminated directly.

The US effect on the photocurrent spectral response of the GaAs substrate was insignificant. At the same time, the sonication of the CdZnTe substrate has resulted in the photosensitivity increase (by a factor of 2 both for integrated value and for absolute maximum) and the change of the spectral distribution of the photocurrent (see figure 3). The photosensitivity of the MBE MCT epilayers was increased slightly, while an essential rise of the photosensitivity of LPE-grown p-type MCT layers took place after the sonication (see figure 4).

Let us consider the US influence on photocurrent spectrums of CdZnTe. Figure 3 shows curves of the photocurrent spectral response. The initial spectrum is a selective peak with the spectral position of the 'red' boundary which corresponds with the band gap $E_g = 1.53$ eV ($x = 0.04$).

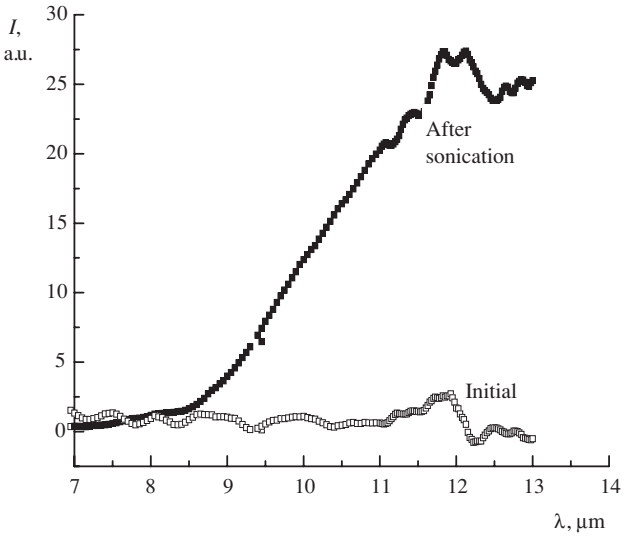

Figure 4. Curves of the photocurrent spectral response for the LPE-grown p-$Hg_{1-x}Cd_xTe$ layer before and after sonication, $T = 78$.

It was used a relation between the band gap of $Cd_{1-x}Zn_xTe$ compound and x [9]:

$$E_g(x) = 1.5045 + 0.631x + 0.128x^2.$$

The 'red' boundary position does not change and the additional energy peak (1.6 eV) emerges after the sonication.

The observed experimental results can be ascribed to sonically stimulated transformation of the point defect system in this material. Recently (by the example of $Cd_{1-x}Mn_xTe$ [10]), it has been shown that the energy transferred by the elastic wave is sufficient for the beginning of the point defect structure transformation that has resulted in the crystal photosensitivity increase. We have suggested that the photosensitivity rise after the sonication of the CdZnTe substrate follows generally from the generation of cationic vacancies, which are acceptors and centres of photosensitivity for CdTe and CdTe-based alloys [11].

It is also known that in the A^2B^6 semiconductor compounds zinc has an intrinsic tendency to form not only substitutional defects but also interstitials. Interstitial zinc, which is a mobile donor defect, usually creates clusters and precipitates at various kinds of macrodefects in the crystal (dislocations, grain boundaries and twins) [8]. One can assume that sonically stimulated cluster dissociation occurs and escape of zinc from sinks results in the formation of a CdZnTe compound with bigger composition in comparison with the matrix. The appearance of the additional energy peak after the sonication is likely to be associated with the macro-inhomogeneity of the solid solution and formation of a CdZnTe mixed structure with a variable band gap between 1.53 eV and 1.6 eV ($x = 0.04$–0.16).

Thus, our study has established the better stability of GaAs substrate parameters against sonication as compared with the CdZnTe substrate that could be connected with the fundamental properties of these materials (for example, the smaller ionicity and the larger stacking fault energy of III–V compounds compared to them in II–VI compounds). It is thought that the used conditions of sonication in our experiment have not likely resulted in the residual transformation of the defect system of GaAs substrates in contrast to CdZnTe substrates, which are an ultrasonically stimulated source of donors and acceptors for MCT epilayers.

4.2. Discussion of the carrier concentration change in MCT thin films.

The above results allow us to make a preliminary conclusion about a significant role of the substrate type for the stability of the MCT epilayers. Let us now consider processes taking place in the epilayer directly.

As was noted previously, immediately after growth MBE-grown MCT layers are n-type; p-type MCT layers are obtained by annealing in consequence of the mercury diffusion from the volume, which remains doped by acceptor-like Hg^- vacancies. Evidently, a similar process occurs during a sonication also as a result of the local heat release due to the absorption of US vibration [12] and the decrease of the ion diffusion activation energy [13]. It could be resulting in the increase of the hole concentration both for MBE and for LPE MCT films. The ultrasonic effect is similar to the process of the natural degradation of MCT in this case.

The sonically stimulated change of the electron component of the conductivity takes place mainly at the expense of the change of the contribution of low-mobility ('heavy') electrons (see table 1). Calculation has shown that heavy electrons are presented in the initial MBE-grown n-type MCT layers. In LPE-grown p-type MCT layers they appear after the first US treatment. After the second sonication their contribution (the value of the characteristic dimension d_{1layer}) increases in both cases. But during isothermal ageing (one year) partial parameter relaxation has occurred. It is also necessary to note that the concentration of 'heavy' electrons exceeds considerably the concentration of 'light' electrons (see table 1).

Heavy electrons are observed both in MCT bulk crystals [14] and in films grown by LPE [15] and MBE [16]. But the reasons for their appearance are not always clear. Low-mobility electrons may be present for the reason of the conduction band bottom modulation, due to random distribution of electrically charged centres giving rise to density-of-states tails [17]. A study of galvanomagnetic phenomena in MBE-grown n-MCT films has shown that the most probable sources of such electrons are surface layers and heterogeneities [18]. For example, the anodic oxide deposited onto the MCT film surface makes the concentration of low-mobility electrons higher and that of anodic fluoride lower [18].

The existence of a surface charge whose density depends on surface treatment is a possible reason for the surface influence on the carrier parameters. At the same time, the inclusion boundaries may well be regions in which the electron mobility is lower. According to the theory of local electroneutrality, a foreign inclusion (or a surface contaminant) shifts the Fermi level in semiconductor at the interface with the inclusion towards the electroneutrality level. In MCT, especially at low CdTe content, the Fermi level lies high in the conduction band, which means that the electron concentration near the inclusion is higher [18].

In conformity with the Granato–Luecke model dislocations move in an ultrasonically loaded crystal

as a vibrating string and selectively absorb the US energy. Considering the prevalence of the sonic-dislocation mechanism of the interaction between the ultrasonic wave and crystal [19], we suggest that dislocations including the surrounding atmosphere of impurities and intrinsic defects could be considered as such inclusions with regions of low-mobility electrons around them, especially since the dislocation presence has also resulted in the conduction band bottom modulation. The increase of the characteristic dimension d_{1ayer} of the layer with 'heavy' electrons could be connected with defect redistribution in dislocation atmospheres as well as transformation of existing extended defects under the action of ultrasonic.

Some experimental results testify in favour of such statements. A thin layer with high density and low mobility of electrons was detected for MCT (similar to ours) films grown by MBE on GaAs substrates near the interface with a CdTe buffer using the method of layer-by-layer etching [20]. TEM images have demonstrated the presence of a network of dislocations near this region. A layer with 'heavy' electrons containing extended defects was detected by similar methods for MCT epitaxial layers subjected to ion milling [21]. Thus, the high density and low mobility of electrons can be attributed to the high defectiveness of detected layers. The analysis of the sonically stimulated appearance of 'heavy' electrons in MCT structures on the basis of the results of structural investigations will be presented in future publications.

4.3. Sonically stimulated effects in bulk MCT crystals

We have also carried out some experiments with bulk MCT ($x = 0.2$) crystals at *in-situ* ultrasonic loading with intensity $W_{US} \sim 10^4$ W m^{-2}. All parameters have been measured during sonication. Their change had a reversible character with a relaxation time of 10^2–10^3 s after switching off the ultrasound.

The effect of US loading manifests itself as an increase of the electron concentration in the impurity–conductivity temperature range ($T < 120^\circ$ K) in n-type MCT crystals and correlates with a value of the extended defect density in samples investigated [7]. A study of the magnetic field dependence of the Hall coefficient for p-type MCT bulk crystals had shown that both sonically stimulated p-to-n conductivity type conversion (figure 5, sample 1) and an absence of the ultrasonic influence (figure 5, sample 2) are observed depending on the density of extended defects in crystal.

It should be also noted that the negative differential resistance region was detected in the *I–V* characteristic measured in n-type MCT bulk crystal at 78 K during US loading (see figure 6). We think this phenomenon could be an experimental evidence of the appearance of 'heavy' electrons and is very attractive in applied respect. However, more experiments are, clearly, necessary.

As clearly shown in figure 6, the phenomenon of the sonically stimulated negative differential resistance is specified by the value of a threshold US power. We also observed the threshold change of the Hall coefficient sign during the sonication of the p-type MCT bulk crystals under a fixed value of the current and magnetic field, when the US power has amounted to the certain value.

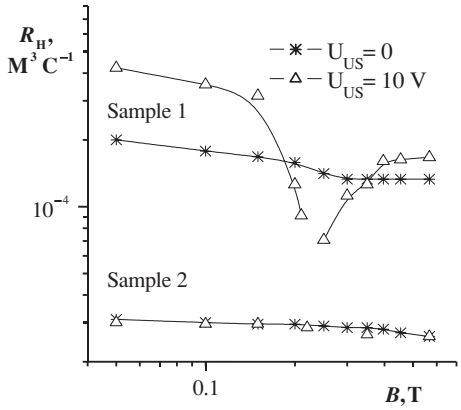

Figure 5. Magnetic field dependences of the Hall coefficient for p-$Hg_{1-x}Cd_xTe$ bulk crystals at 78 K with the starting value of the dislocation density: 1—10^9 m^{-2}, 2—10^8 m^{-2}. U_{US} is the amplitude of the electric field applied to the US transducer.

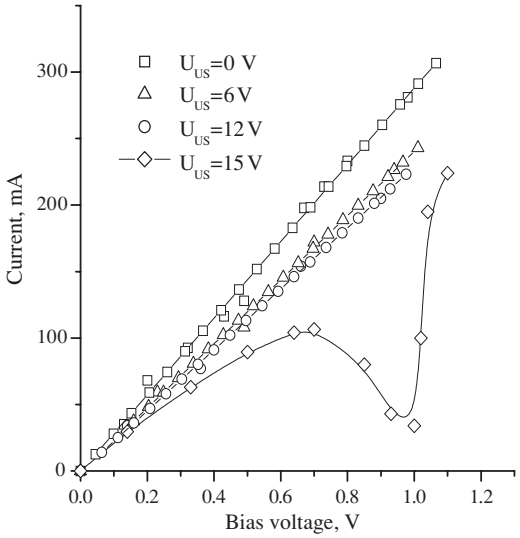

Figure 6. *I–V* characteristics of the $Hg_{1-x}Cd_xTe$ bulk crystal at 78 K with a negative differential resistance region; U_{US} is the amplitude of the electric field applied to the US transducer. The dislocation density is 10^{10} m^{-2}.

Thus, experiments carried out with bulk MCT crystals at *in-situ* ultrasonic loading confirm the decisive role of dislocations for sonically stimulated effects in this material. The dislocation contribution to the change on MCT properties clearly appears [22–24]. Moreover, the electrical properties of dislocations are mainly determined by their extrinsic effects, such as a change or redistribution in the surrounding atmosphere of point defects, which has a donor-like character, rather than by the intrinsic ones due to their dangling bonds [25]. Really since a suitable investigation has made it clear that the dislocation density has not increased during *in-situ* US influence in our experiment, it could be suggested that the phenomena observed are related with the redistribution of point defects in the dislocation atmospheres of the crystal. The threshold character of the material properties change is conditioned by the overcoming of a certain barrier for the beginning of the defect system transformation. In particular,

the absorption of the acoustic energy by dislocations during US influence has resulted in electrical activation of donor-like point defects 'bounded' at extended defects, which was discussed in detail elsewhere [26]. As a consequence, the increase of the electron component of the conductivity occurs. Obtained values of the relaxation time of the electron concentration for bulk MCT samples after switching off the US loading at *in-situ* measurements confirm the ionic nature of the ultrasonically stimulated processes.

5. Conclusion

From the analysis of the magnetic field dependent Hall data, parameters of the charge carrier transport in LPE and MBE MCT layers were determined prior to and after the sonication. We have demonstrated that the action of the high-frequency deformation excited in MCT epilayers by a piezo-transducer results in a change of the carrier concentration up to the conductivity type conversion. The best agreement between experiment and calculation was obtained assuming that the layer with 'heavy' electrons was formed as a consequence of the sonication. We suggest that dislocations including the surrounding atmosphere of impurities and intrinsic defects could be considered as inclusions with regions of low-mobility electrons around them.

A comparison of the experimental results, which were obtained from the investigation of MCT alloy parameters during US treatment and after sonication, has shown their correlation. The increase of the electron contribution to the conductivity of n-MCT, the change of the conductivity type of p-MCT and the 'heavy' electrons appearance under US influence both for bulk crystals and for epilayers have confirmed that these phenomena are an inherent property of MCT itself irrespective of the preparation technique or treatment manner.

At the same time, the experimental data clearly show that the parameters of MCT thin films grown by MBE on GaAs substrates are more stable to the sonication than MCT thin films grown by LPE on CdZnTe substrates. Substrate properties have been observed to play a significant role for the stability of the MCT epilayers.

Acknowledgments

The authors are grateful to S A Dvoretsky, Yu G Sidorov and N N Mikhailov for supplying MBE grown MCT films.

References

[1] Rogalski A 2000 *Infrared Detectors* (Amsterdam: Gordon and Breach) p 681
[2] Varavin V S, Dvoretsky S A, Liberman V I, Mikhailov N N and Sidorov Yu G 1995 *Thin Solid Films* **267** 121
Varavin V S, Dvoretsky S A, Liberman V I, Mikhailov N N and Sidorov Yu G 1996 *J. Cryst. Growth* **159** 1161
[3] Myslivets K A and Olikh Ya M 1990 *Fiz. Tverd. Tela* **32** 2912
Myslivets K A and Olikh Ya M 1990 *Sov. Phys. Solid State* **32** 1692
[4] Beer A C 1963 *Galvanomagnetic Effects in Semiconductors* (New York: Academic)
[5] Voitsekhovskii A V, Kokhanenko A P, Korotaev A G, Grigor'ev D V, Varavin V S, Dvoretsky S A, Sidorov Yu G and Mikhailov N N 2003 *Proc. SPIE* **5136** 411
[6] Sizov F F, Lysiuk I O, Gumenjuk-Sichevska J V, Bunchuk S G and Zabudsky V V 2006 *Semicond. Sci. Technol.* **21** 358
[7] Savkina R K and Vlasenko A I 2002 *Phys. Status. Solidi.* b **229** 275
[8] Lisiansky M, Korchnoi V, Nemirovsky Y and Weil R 1997 *J. Phys. D: Appl. Phys.* **30** 3203
[9] Tobin S P *et al* 1995 *J. Electron. Mater.* **24** 697
[10] Savkina R K, Sizov F F and Smirnov A B 2006 *Semicond. Sci. Technol.* **21** 152
[11] Lany S, Ostheimer V, Wolf H and Wichert Th 2001 *Physica* B **308** 958
[12] Savkina R K and Smirnov A B 2005 *Infrared Phys. Technol.* **46** 388
[13] Krevchik V D, Muminov R A and Yafasov A Ya 1981 *Phys. Status. Solidi.* a **63** K159
[14] Finkman E and Nemirovsky Y 1982 *J. Appl. Phys.* **53** 1052
[15] Leslie-Pelesky D L, Seiler D G, Loloee M R and Littler G L 1987 *Appl. Phys. Lett.* **51** 1916
[16] Antoszewski J and Faraone L 1996 *J. Appl. Phys.* **80** 3881
[17] Brudnyu V N, Grinyaev S N and Stepanov V E 1995 *Physica* B **212** 429
[18] Varavin V S, Kravchenko A F and Sidorov Yu G 2001 *Semiconductors* **35** 992
[19] Hirth J P and Lothe J 1967 *Theory of Dislocations* (New York: McGraw-Hill) chapter 16
[20] Bakhtin P A, Dvoretski S A, Varavin V S, Korobkin A P, Mikhalov N N and Sidorov Yu G 2004 *Semiconductors* **38** 1168
[21] Bogoboyashchyy V V, Iznin I I, Mynbaev K D, Pociask M and Vlasov A P 2006 *Semicond. Sci. Technol.* **21** 116
[22] Shin S H, Arias J M, Zandian M, Pasko J G and DeWames R E 1991 *Appl. Phys. Lett* **59** 2718
[23] Johnson S M, Rhiger D R, Rosbeck J P, Peterson J M, Taylor S M and Boyd M E 1992 *J. Vac. Sci. Technol.* **10** 1499
[24] List R L 1992 *J. Vac. Sci. Technol.* **10** 1651
[25] Renault P O, Barbot J F, Giault P, Declemy A, Rivaud G and Blanchard C 1995 *J. Physique* III **5** 1383
[26] Olikh Ya M, Savkina R K and Vlasenko O I 1999 *Semiconductors* **33** 398